

AURORAL OVAL AND POLAR SUBSTORMS OBSERVED
BY A SATELLITE AND GROUND-BASED
OBSERVATIONS IN ANTARCTICA

T. NAGATA*, T. HIRASAWA* and M. AYUKAWA*

Abstract: The morphology of the “discrete” and “diffuse” auroral belts in the southern polar region is statistically examined as a function of geomagnetic Kp -index, using USAF-DAPP auroral photographs.

Results of the statistical analyses are summarized in Fig. 9, which indicates the following characteristics of the two auroral belts.

(a) The discrete auroral belt is always located on the poleward side of the diffuse auroral one.

(b) The discrete auroras are observed mostly in the evening-to-midnight sectors, whereas the diffuse auroras are dominant in the midnight-to-early morning sectors.

(c) The discrete auroras are observable in the evening sector even when Kp -index is very low; the discrete auroral belt in such a case is identified to the so-called auroral oval.

(d) The discrete auroral belt approaches to a circular shape along 71° – 72° in geomagnetic latitude when Kp -index approaches $Kp \geq 5$.

(e) The diffuse auroral belt is confined to the night-side sectors during the geomagnetically quiet period, but it expands towards the evening sector along a geomagnetic latitude circle of 68° – 69° , accompanied by a rapid expansion of width, in association with increasing Kp -index.

Comparisons of DAPP auroral photographs and all-sky camera ones with scanning auroral spectrophotometric data on ground for H_β 4861 Å and OI 5577 Å emission lines have identified the discrete and diffuse auroral belts to the electron and proton auroral belts respectively.

1. Introduction

Since the time of IGY-IGC, auroral forms observable from a station have been photographed by the all-sky camera technique. Based on morphological studies in detail of the all-sky camera photographs obtained at many stations distributed over the north and south polar regions, the concept of auroral substorm and that of auroral oval have been established (*e.g.* AKASOFU, 1964, 1968; FELDSTEIN and STARKOV, 1967).

On the other hand, epoch-making and striking observations of auroral morphology have recently been carried out by ISIS-II and USAF-DAPP polar-orbiting

* National Institute of Polar Research, 9–10, Kaga 1-chome, Itabashi-ku, Tokyo 173.

satellites (LUI and ANGER, 1973; PIKE and WHALEN, 1974). One of the most significant results of morphological studies on auroras observed by the satellites would be a clear distinction between a fairly uniform belt of diffuse aurora and discrete and bright auroras which lie along the FELDSTEIN's auroral oval. The diffuse auroral belt is sharply defined at its equatorward edge, which is located at about 65° in invariant latitude in the midnight sector, and the diffuse auroral belt is relatively unaffected by individual magnetospheric substorms, even when the discrete auroras show the drastic poleward movement at the breakup phase of auroral substorm (LUI and ANGER, 1973). LUI *et al.* (1973) have further noted that the diffuse aurora appears sometimes to split up into two branches, one along the auroral oval and the other along a constant geomagnetic latitude circle. PIKE and WHALEN (1974) have concluded from the DAPP auroral photographs that the distributions of discrete auroras in the DAPP photographs further substantiate the concept of FELDSTEIN's auroral oval as well as that of AKASOFU's auroral substorm. Using the satellite data, however, SNYDER *et al.* (1974) and SNYDER and AKASOFU (1974) have modified the original pattern of AKASOFU's auroral substorm which had been obtained based on the all-sky camera data only; a revised auroral substorm pattern at the maximum activity of substorm has been presented mostly based on the satellite data.

Although the auroral imaginary photographs taken by satellites have much contributed to the progress of auroral studies in various ways as mentioned above, very little statistical examinations of these auroral photographs have been carried out to date. The main aim of the present paper is therefore to statistically examine the morphological characteristics of the discrete and diffuse auroral belts as dependent on the geomagnetic activity and as a function of the local time. 350 sheets and some more of USAF-DAPP satellite photographs taken during the period from May 1 to June 30, 1973 over the southern polar region have been analyzed in the present work in comparison with the ground-based auroral data simultaneously obtained at Syowa Station in Antarctica by two of the present authors (T.H. and M.A.). As general characteristics of the imaginary DAPP auroral photographs themselves have already been described in detail in the PIKE and WHALEN paper (1974), they will not be re-stated in the present paper.

2. Distinction between Discrete and Diffuse Auroras

It has already been reported that the discrete auroral belt and the diffuse auroral one can be definitely distinguished from each other in the ISIS-II and DAPP auroral photograph data (LUI and ANGER, 1973; LUI *et al.*, 1973; PIKE and WHALEN, 1974; SNYDER and AKASOFU, 1974).

Fig. 1 shows an example of DAPP auroral imaginary photograph taken under a moderately disturbed condition ($Kp=4$) in the southern polar region, where

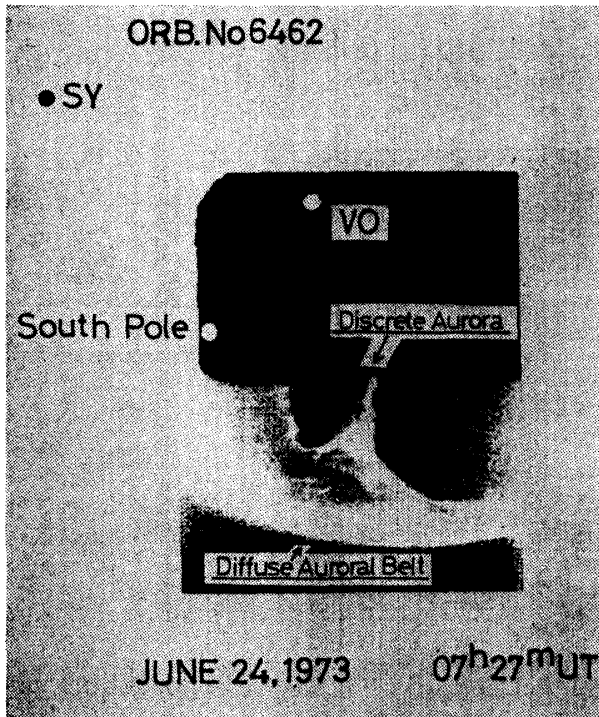


Fig. 1. An example of DAPP auroral photograph to show a distinction between the discrete auroral belt and the diffuse auroral one ($Kp=4$).

SY: Syowa Station (Geomag. lat= $69.6^{\circ}S$, Geomag. long= $77.1^{\circ}E$)
 VO: Vostok Station (Geomag. lat= $89.2^{\circ}S$, Geomag. long= $77.8^{\circ}E$)

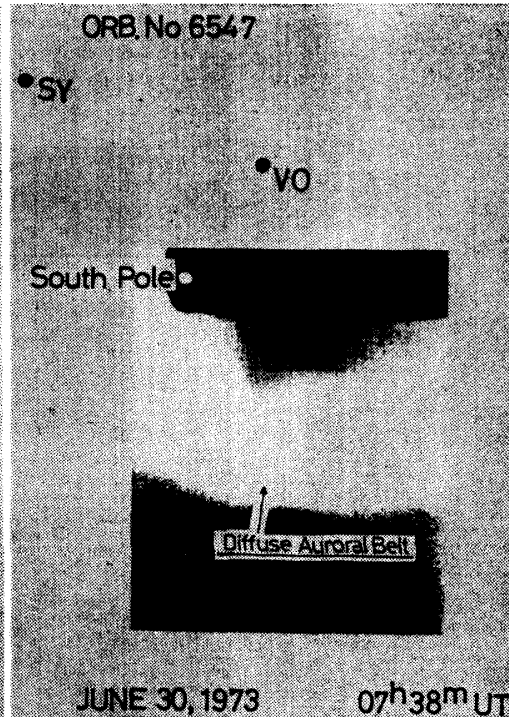


Fig. 2. An example of DAPP auroral photograph to represent an active diffuse auroral belt during a geomagnetically active period ($Kp=5$).

locations of the South Pole, Syowa Station (SY) and Vostok (VO) are indicated. In the midnight sector in this auroral photograph, discrete auroras can be clearly separated from a diffuse auroral belt. Dynamical characteristics of the discrete auroras are definitely different from those of the diffuse auroral belt. Namely, the discrete auroras begin to develop polewards from the poleward boundary of the diffuse auroral belt and to propagate towards the evening side (*i.e.* the westward traveling surge phenomenon, AKASOFU, 1968), whereas the diffuse auroral belt of about 3° in latitudinal width remains steadily along a geomagnetic latitude circle belt, its sharply defined equatorward edge being constantly located at geomagnetic latitude $\Phi_m=65^{\circ}$.

Fig. 2 shows a typical example of DAPP auroral photograph to represent an active diffuse auroral belt during a geomagnetically active period ($Kp=5$). During the active period, the belt steadily stays between 60° and 70° in the midnight sector and the dependence of diffuse auroral characteristics upon the geomagnetic

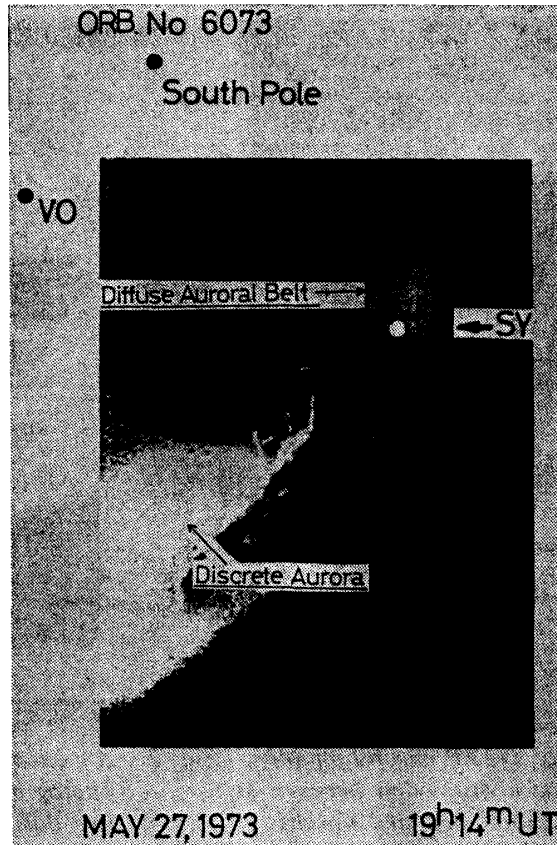


Fig. 3. An example of DAPP auroral photographs to represent a marked extension of a diffuse auroral belt from the midnight sector towards the early evening side in association with an increasing geomagnetic activity ($Kp=3$).

activity is represented by an increase of auroral brightness and an expansion of auroral belt width in association with an increase in geomagnetic activity. It may be further noted in Fig. 2 that the equatorward boundary of the diffuse auroral belt is much sharper than its poleward boundary.

Fig. 3 shows a characteristic diffuse auroral belt which is markedly extended from the midnight sector toward the early evening side in association with a moderate geomagnetic activity ($Kp=3$).

Figs. 4 and 5 show two examples of an auroral morphological condition that no diffuse aurora is observable in the midnight and evening sectors corresponding to a geomagnetically quiet period ($Kp \leq 2$). In Fig. 4, for example, discrete auroras take place approximately along the auroral oval from the midnight sector to the early evening one, associated with a westward traveling surge of a large scale in the late evening sector. However, no diffuse auroral belt can be directed throughout the whole photographed area. In Fig. 5 also, the multi-fold appearance

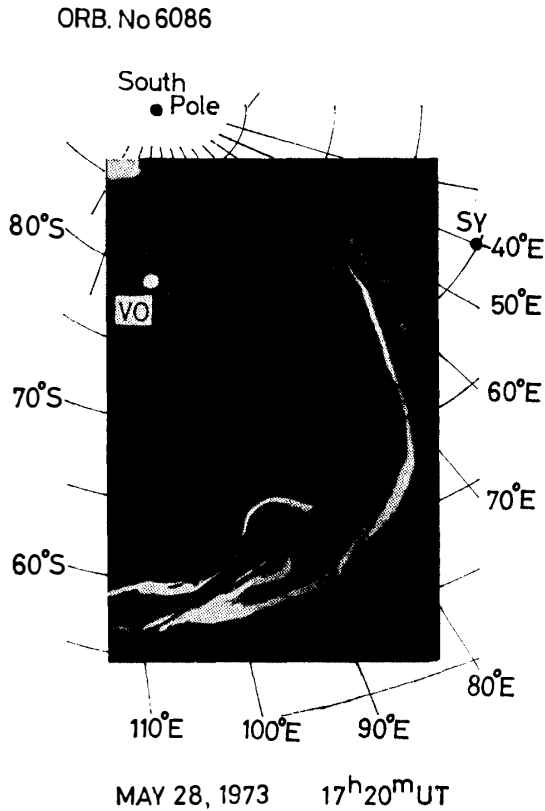


Fig. 4. Example of DAPP auroral photograph to represent a geomagnetically quiet condition when only discrete auroras with a westward traveling surge are present and no diffuse auroral belt is observed ($K_p=2$).

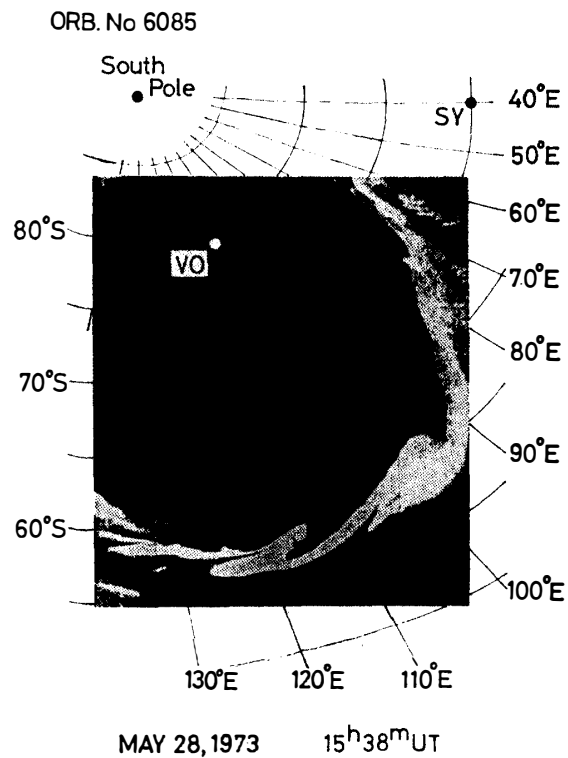


Fig. 5. Example of DAPP auroral photograph to show only multi-fold appearance of discrete auroras and no appreciable diffuse aurora under the geomagnetically quiet condition ($K_p=2$).

of discrete auroral surges is clearly observed, but any significant diffuse auroral belt cannot be found.

As illustrated in these typical examples of DAPP auroral photographs, individual auroras observed from satellites can be generally classified into two different groups, namely "discrete" aurora and "diffuse one". When the discrete and diffuse auroras co-exist, the diffuse auroral belt is always located on the equatorward side of the discrete auroras. When the magnetospheric disturbance activity is very low so that no polar magnetic substorm is observed, only discrete auroras are present and no diffuse auroral belt takes place at least in the evening and early evening sectors in the polar region. In some rare cases, however, a definite distinction between the discrete and diffuse auroras is slightly difficult in the DAPP auroral photographs.

3. Occurrence Characteristics of Discrete and Diffuse Auroras

As summarized in the previous section, only discrete auroras are observable in the evening sector under the quiet condition, whereas the diffuse auroral belt extends from the midnight sector to the early evening one during a geomagnetically disturbed period. It appears thus that the occurrence characteristics of the discrete and diffuse auroras are significantly dependent on the polar geomagnetic activity as well as on the geomagnetic local time.

The dependence of occurrence frequency of the discrete and diffuse auroras upon the geomagnetic local time is statistically examined with 350 DAPP auroral photographs, the resultant histograms being shown in Fig. 6. In the figure, the percentages of appearances of no aurora, discrete aurora only, both discrete and diffuse auroras, and diffuse aurora only are graphically represented for five geomagnetic time sectors, *i.e.* the early morning (3 hours around 03^h in geomagnetic local time), the midnight (around 00^h), the late evening (around 21^h), the evening (around 18^h) and the early evening (around 15^h) sectors. It may be observed in the histograms that the diffuse aurora is most frequently observed around the midnight (*i.e.* 21^h–03^h), its occurrence frequency systematically increasing with geomagnetic local time from the early evening towards the early morning. On the other hand, the occurrence of the discrete auroras is dominant in the early evening and evening sectors and the share of their appearance gradually decreases with time from 95% at 15^h to 46% at 03^h. Statistically speaking, therefore, the discrete auroras may be considered the midnight-to-evening side phenomena, while the diffuse auroras are the midnight-to-morning side ones.

To statistically study the dependence of auroral occurrence on the geomagnetic activity as well as on the geomagnetic local time, all data of the occurrence

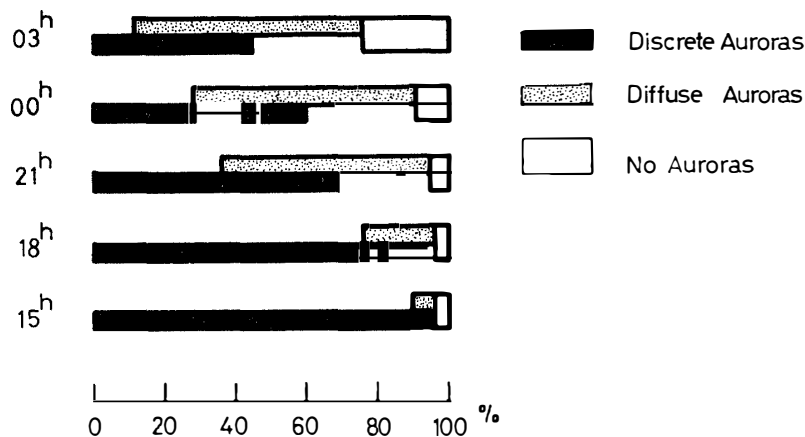


Fig. 6. Occurrence frequency histograms of the discrete and diffuse auroras as dependent on the geomagnetic local time.

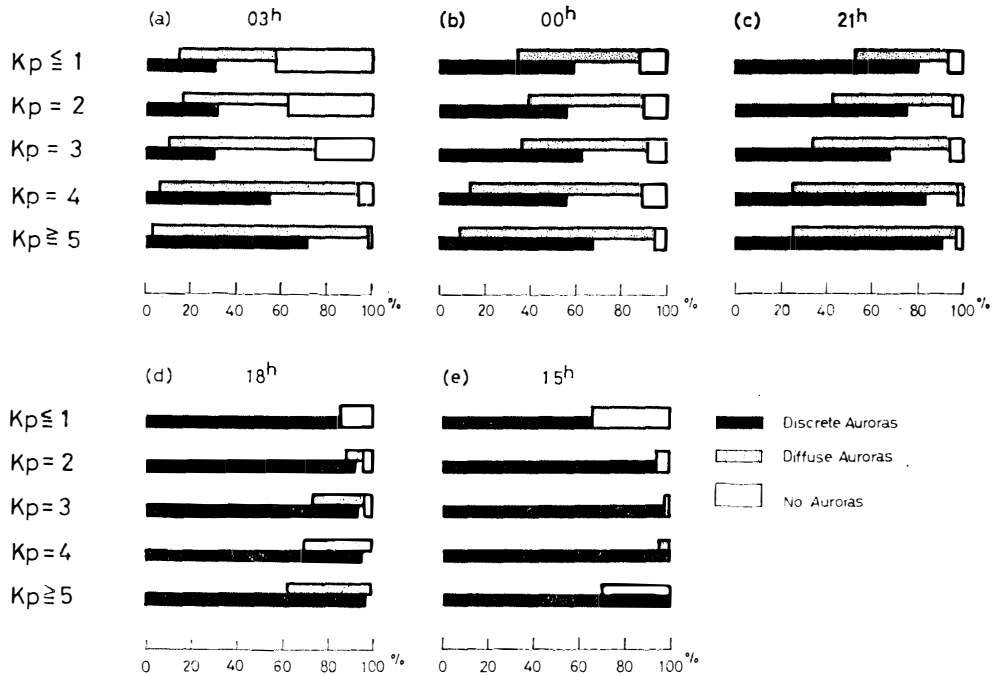


Fig. 7. Occurrence frequency histograms of the discrete and diffuse auroras as dependent on the geomagnetic local time as well as on geomagnetic Kp -index.

frequencies of the discrete and diffuse auroras used for deriving Fig. 6 have been rearranged separately for different magnitudes of geomagnetic Kp -indices, the result being shown in Fig. 7. It can be observed in this figure that the occurrence frequency of the diffuse auroras always increases with increasing geomagnetic activity at any local time. In the early morning (03^h), midnight (00^h) and late evening (21^h) sectors, the diffuse aurora can be observed with a considerable probability even when the geomagnetic activity is very low ($Kp \leq 1$). At the evening hour (18^h), however, the diffuse aurora cannot be observed under the quiet geomagnetic condition ($Kp \leq 1$), but it begins to appear at $Kp=2$ and its occurrence frequency increases with an increase of Kp -index, reaching about 40% for $Kp \geq 5$. In the 15^h geomagnetic local time sector, the diffuse aurora does not take place for a wide range of low geomagnetic activity ($Kp \leq 3$).

The occurrence characteristics of the diffuse auroras, summarized in Fig. 7, may indicate that the diffuse auroral belt gradually extends from the midnight sector towards the early evening one with an increase in the geomagnetic activity represented by Kp -index. A pictorial example of the extended diffuse auroral belt is well demonstrated in Fig. 3.

As illustrated in Fig. 7, the discrete auroras are most frequently observed in the early evening to the late evening sectors (15^h–21^h) even during the quiet geomagnetic condition. The occurrence frequency of discrete auroras occupies

more than 90% in the early evening and evening sectors when $Kp \geq 2$. In the late evening and midnight sectors, the appearance probability of discrete aurora considerably exceeds 50% even for the geomagnetically quietest condition ($Kp \leq 1$). In other words, it is very seldom that no discrete aurora appears in the early evening to late evening sectors as far as $Kp \geq 2$. This feature is pictorially demonstrated in individual auroral patterns shown in Figs. 4 and 5.

4. Configuration and Development Pattern of Discrete and Diffuse Auroral Belts as Dependent on Geomagnetic Activity

Based on the results of extensive analyses of the all-sky camera data of auroras obtained at a widely spread network of polar observatories, FELDSTEIN (1963) and FELDSTEIN and STARKOV (1967) have studied the morphology and dynamics of auroral belt and have statistically derived the concept of "auroral oval". In the present study which deals with the distribution patterns of both discrete and diffuse auroral belts, the problem of auroral oval may have to be re-examined from the new viewpoint that there are clearly distinguishable two auroral belts; namely, discrete and diffuse auroral belts.

The polar distance of the poleward and equatorward boundaries of the discrete and diffuse auroral belts from the geomagnetic pole are scaled individually on DAPP auroral photographs at four geomagnetic meridian sectors, 15^h, 18^h, 21^h and 00^h, for different geomagnetic activities represented by Kp -index. The statistical results of the locations of discrete and diffuse auroral belts thus obtained are given in Fig. 8, where the vertical length of individual bars represents the width of the respective auroral belts at given times for given Kp -indices.

In Fig. 8(a), characteristic features of the discrete auroral belt dependent on the geomagnetic activity and the geomagnetic local time, such as briefly summarized in the following, may be concluded.

a) When the geomagnetic activity is low, the average polar distance of the discrete auroral belt is largely dependent on the geomagnetic local time; it is about 82° in geomagnetic latitude at 15^h, about 79° at 18^h and about 72° at 21^h and 00^h for $Kp \leq 1$. This systematic time-dependent variation of the average location of the discrete auroral belt can almost exactly represent the FELDSTEIN's auroral oval.

b) With an increase of Kp -index, the discrete auroral belt in the early evening-evening sectors rapidly shifts towards the equator, whereas that in the late evening-midnight sectors is kept approximately invariant at about 72°–73° in geomagnetic latitude; thus the average polar distance of the discrete auroral belt tends to converge towards its approximately constant value in the midnight sector, *i.e.* 72°, when Kp -index reaches or exceeds $Kp=5$. Approximately speaking, therefore, the shape of the discrete auroral belt in the polar region in the afternoon

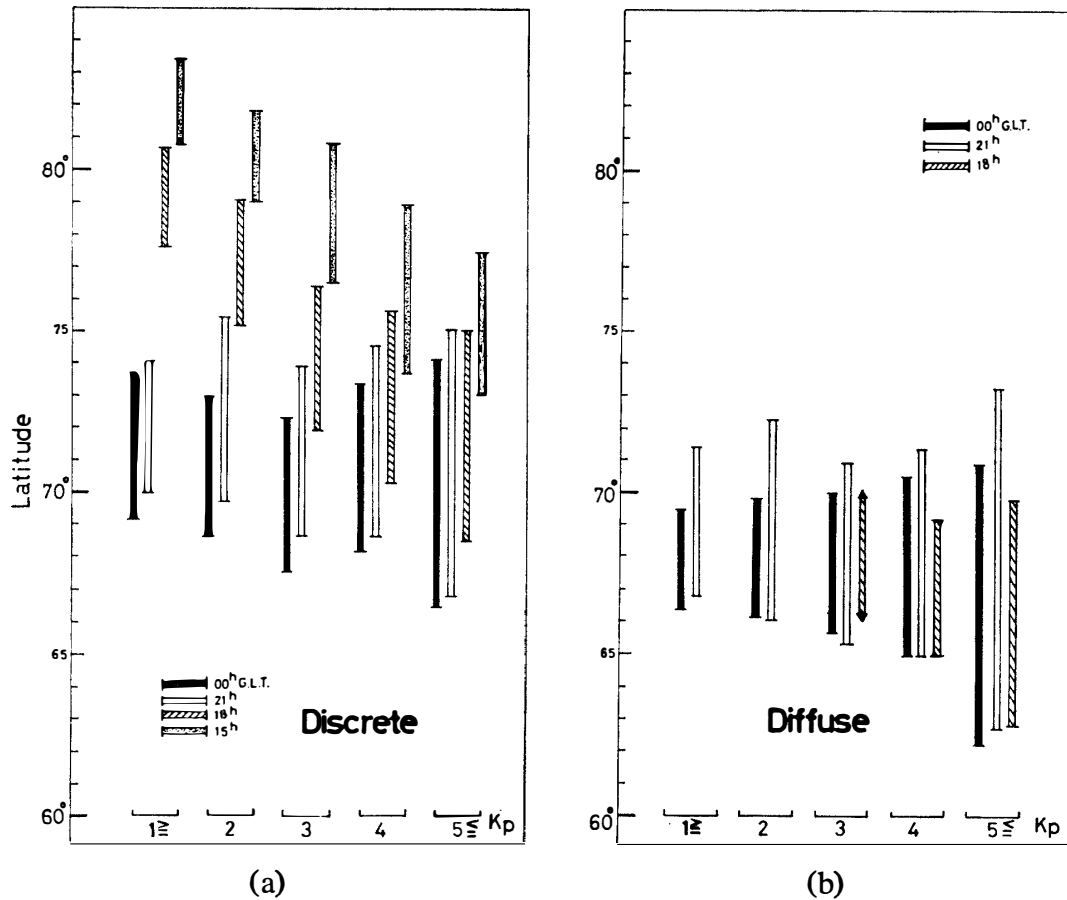


Fig. 8. Average location of the poleward and equatorward boundaries of the discrete auroral belt (a) and the diffuse one (b) as dependent on the geomagnetic local time and geomagnetic Kp -index.

hemisphere (from 15^h to 00^h in geomagnetic local time in the present study) tends to change with an increase of the geomagnetic activity from an oval to a circle of about 20° in polar radius.

c) The width of the discrete auroral belt gradually increases with an increase of Kp -index; namely, from 4.8° to 8.0° at 00^h, from 4.2° to 8.2° at 21^h, from 3.0° to 6.0° at 18^h and from 2.5° to 4.5° at 15^h, corresponding to an increase of Kp -index from the minimum value, $Kp \leq 1$, to the maximum one, $Kp \geq 5$.

The dependence of the average location and width of the diffuse auroral belt on Kp -index at different geomagnetic local times is shown in Fig. 8(b). From the statistical results given in the figure, the following characteristics of the diffuse auroral belt could be summarized.

a) In general, the diffuse auroral belt is located on the equatorward side of the discrete auroral belt.

b) The average location of the diffuse auroral belt remains practically constant at 68° – 69° in geomagnetic latitude regardless of the geomagnetic activity.

c) The equatorward boundary of the diffuse auroral belt systematically shifts towards the lower latitude with increasing geomagnetic activity; namely, from 66.5° for $Kp \leq 1$ to 62.0° for $Kp \geq 5$. On the other hand, the poleward boundary of the belt is considerably different for different geomagnetic local times.

d) The width (W) of the diffuse auroral belt rapidly expands with an increase of Kp -index; for example, $W=3.6^{\circ}$ for $Kp \leq 1$ and $W=9.6^{\circ}$ for $Kp \geq 5$ at 00^{h} . It can also be noted that W -value at 21^{h} is always larger than that at 00^{h} .

e) As already described in the previous section, the diffuse aurora cannot be observed at 18^{h} meridian under the quiet geomagnetic condition ($Kp \leq 1$), and it begins to appear at $Kp=2$. When the diffuse auroral belt appears in the 18^{h} sector, its location is nearly the same as that of the midnight-side (at 00^{h}) belt, *i.e.* about 68° – 69° . This tendency coincides with the observed fact that the diffuse

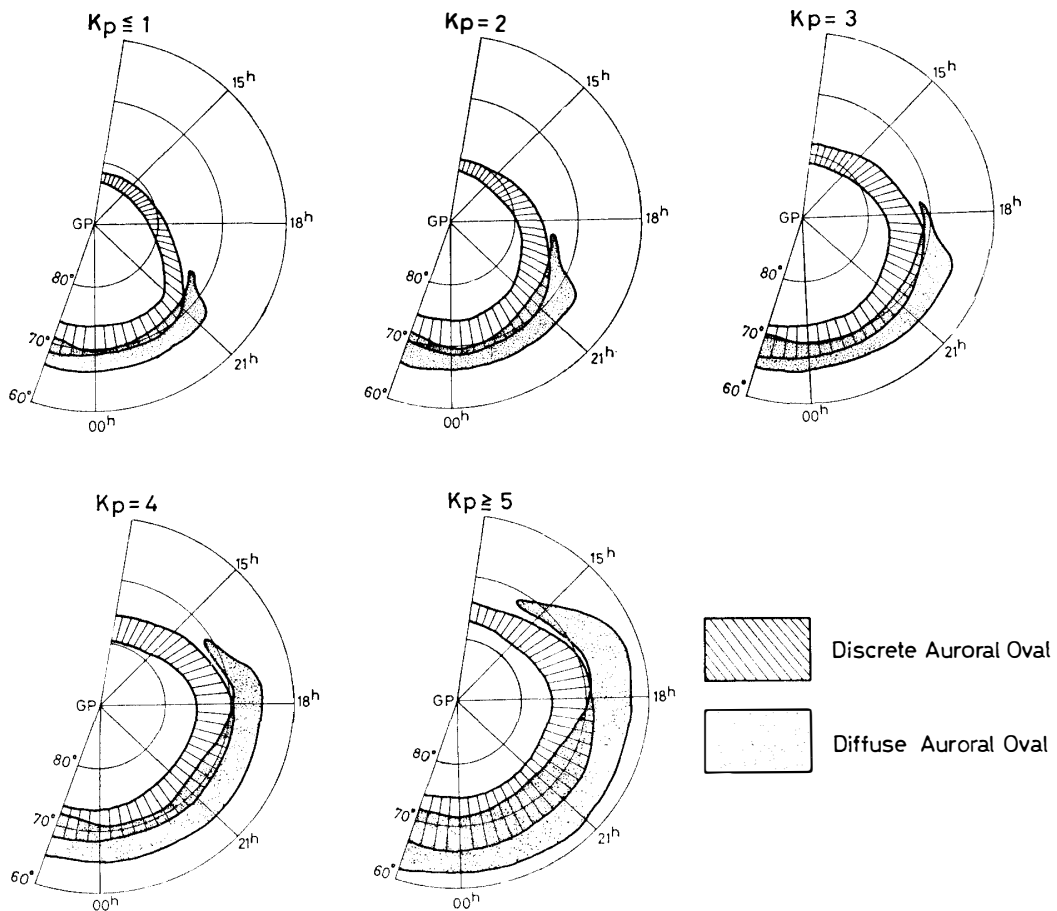


Fig. 9. Schematic illustration of the configuration of the discrete and diffuse auroral belts as dependent on geomagnetic Kp -index.

auroral belt gradually extends from the midnight sector towards the evening one along a latitude circle of 68° – 69° in association with an increase in geomagnetic activity.

Based on the results of the present statistical studies on the occurrence characteristics and the location of the auroral belts of the two types together with the geographical morphology of auroral appearance in individual DAPP auroral photographs, the configuration and development pattern of the discrete and diffuse auroral belts in the southern polar region in the afternoon hemisphere (from 12^h through 18^h to 03^h) have been schematically summarized in Fig. 9 for different degrees of geomagnetic activity. The shape and location of the discrete auroral belt and their dependence on the geomagnetic activity well represent those of the FELDSTEIN's auroral oval, which have been derived from all-sky camera data. We may conclude therefore that the auroral oval, proposed by FELDSTEIN (1963) and confirmed by AKASOFU (1964), represents the discrete auroral belt.

On the other hand, the existence of the diffuse auroral belt has already been pointed out by LUI *et al.* (1973) based on satellite auroral photograph data. The present statistical study based on DAPP auroral photograph data, summarized in Fig. 9, has further clarified general characteristics of the diffuse auroral belt separately from those of the discrete auroral one. Then, the two different types of auroral belt, "discrete" and "diffuse", may have to be caused by different physical mechanisms.

5. Identification of Discrete and Diffuse Auroral Belts

Based on a large number of data of the ground-based spectrophotometric observations of aurora, different types of aurora have been clearly defined to date. They are, (a) the discrete and diffuse electron auroras which are frequently observed during the breakup and post-breakup phases of polar substorms (*e.g.* AKASOFU, 1968; HIRASAWA and NAGATA, 1972), (b) the proton auroras (*e.g.* EATHER and SANDFORD, 1966; FUKUNISHI, 1973) and (c) the OI 6300 Å red electron aurora which appear in higher altitudes (200–300 km in height) only under the quiet geomagnetic condition. Then, a comparison of satellite photographs of aurora with the simultaneous auroral data obtained by the ground-based observations may be able to lead to a physical identification of the discrete and diffuse auroral belts.

In Fig. 10(a), for example, a DAPP auroral photograph is shown together with the simultaneous ground-based all-sky camera photographs obtained at Syowa Station. In this figure, the width of satellite photograph (top) is 1,750 km, while the diameter of all-sky camera photographs (bottom) corresponds to about 1,000 km, so that a mutual comparison of the geographical distributions of auroral luminosity between the satellite and ground-based photographs can be

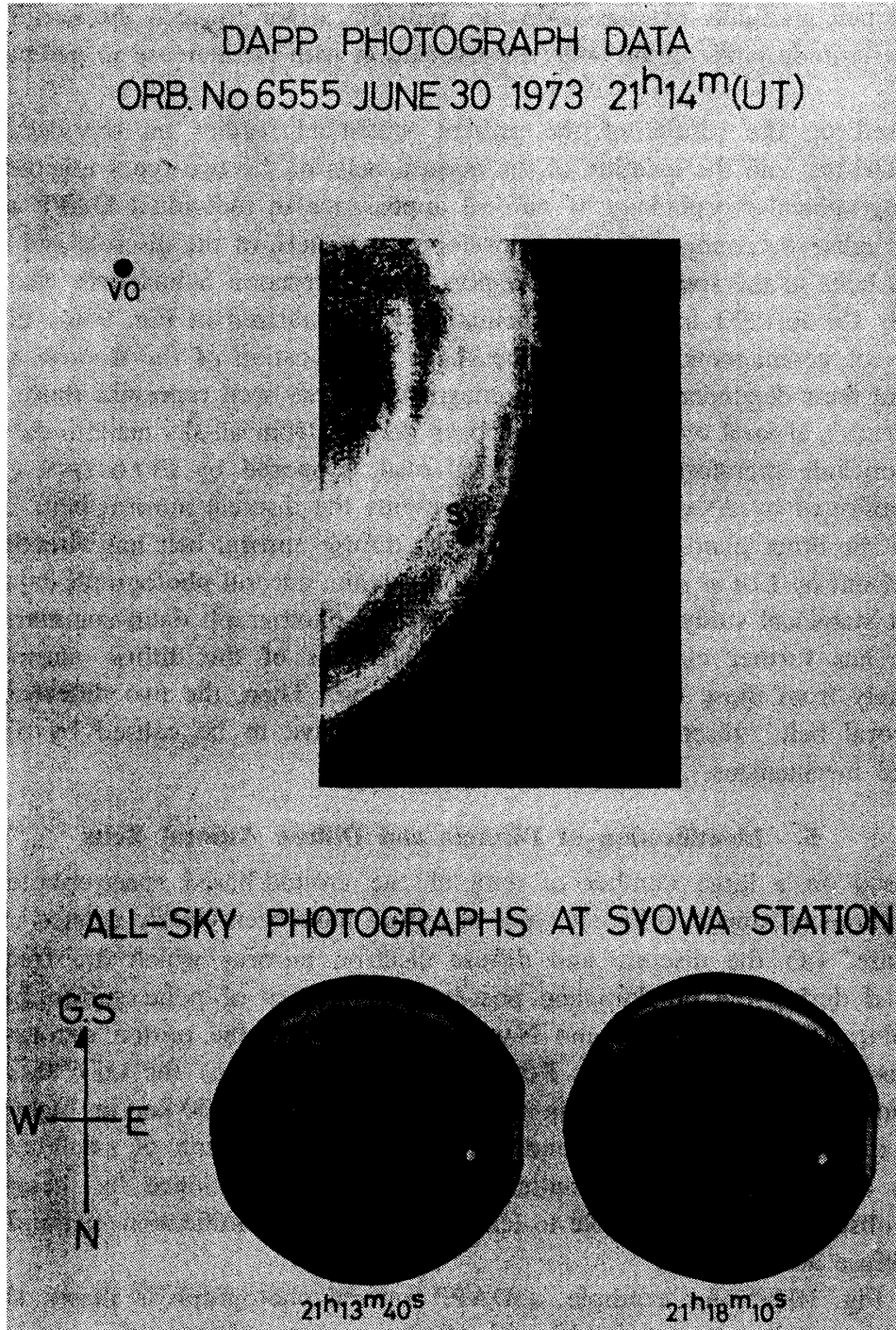


Fig. 10(a). DAPP auroral photograph and simultaneous all-sky camera photographs obtained at Syowa Station.

The radius of the all-sky photograph corresponds to about a quarter of the distance between Syowa Station (SY) and Vostok (VO) on the DAPP photograph.

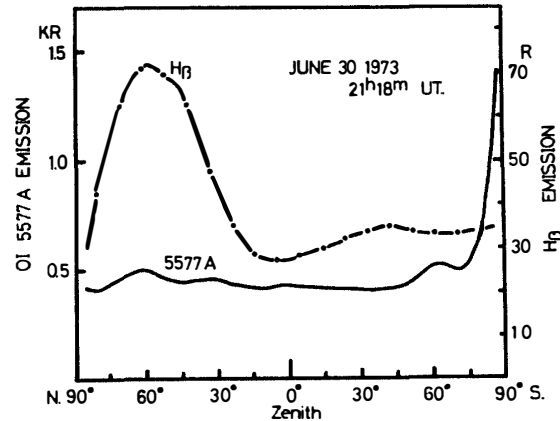


Fig. 10(b). Space distribution along the geomagnetic meridian of intensities of $H\beta$ 4861 Å and OI 5577 Å auroral emissions observed at Syowa Station at the practically same time as that for auroral photographs in Fig. 10(a) ($K_p=5$).

made with a reasonably good resolution. The DAPP photograph indicates that Syowa Station (SY) was located under a diffuse auroral belt which extended from the midnight sector towards the evening one, whereas discrete auroral belts were activated on the poleward side of SY point. The simultaneous all-sky photographs show that faint diffuse auroras with multi-arc structure covered the northern (equatorward) parts of the sky, whereas a bright auroral arc was observed above the southern (poleward) horizon.

In comparing the DAPP photograph with the all-sky camera ones, it may be indicated that the diffuse auroral belt in the DAPP photograph consists of several faint diffuse auroral arcs and the bright auroral arc above the southern horizon in the all-sky records corresponds to the active discrete auroral belt in the DAPP photograph.

The identification of physical characteristics of the diffuse and discrete auroral belts could be obtained from simultaneous data of the auroral spectrophotometry. A geomagnetic north-south scanning spectrophotometer has been operated at Syowa Station for recording the space-time variations of auroral luminosity of $H\beta$ and OI 5577 Å lines which are the typical emission lines excited by the precipitating protons and electrons respectively. In Fig. 10(b), is shown the space distribution along the geomagnetic meridian of auroral luminosity of $H\beta$ and OI 5577 Å emission lines obtained at Syowa Station at the time when the DAPP and all-sky photographs in Fig. 10(a) were taken. In this case, the distance between 85° in N and 85° in S in angle is approximately equivalent to 1,000 km. A comparison of Fig. 10(b) with the all-sky camera photographs in Fig. 10(a) indicates that the faint diffuse auroral belt in the northern sky of Syowa Station can be identified to a broad peak of $H\beta$ intensity, whereas the discrete auroral

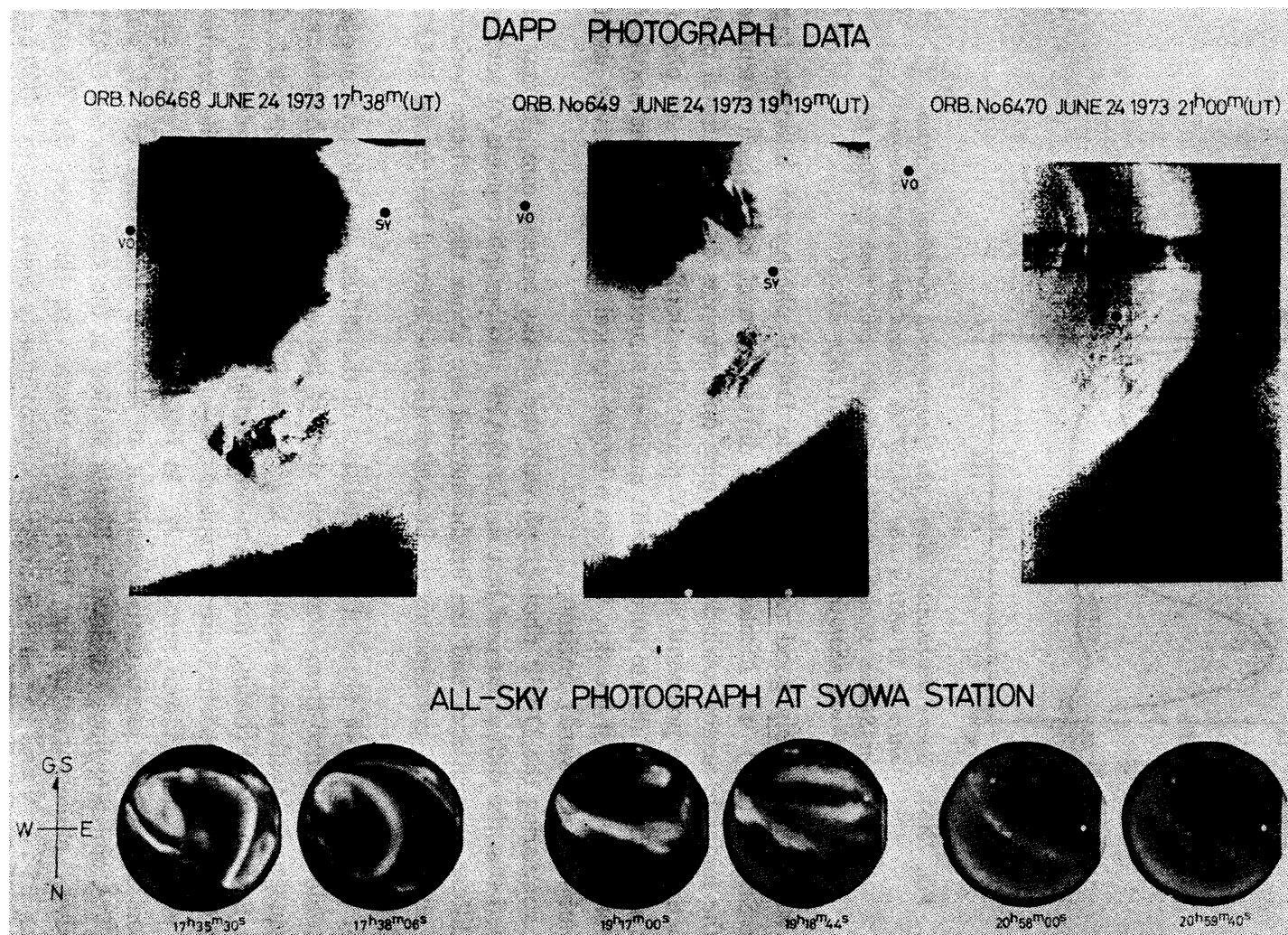


Fig. 11(a). Three successive DAPP auroral photographs and simultaneous all-sky camera photographs obtained at Syowa Station.

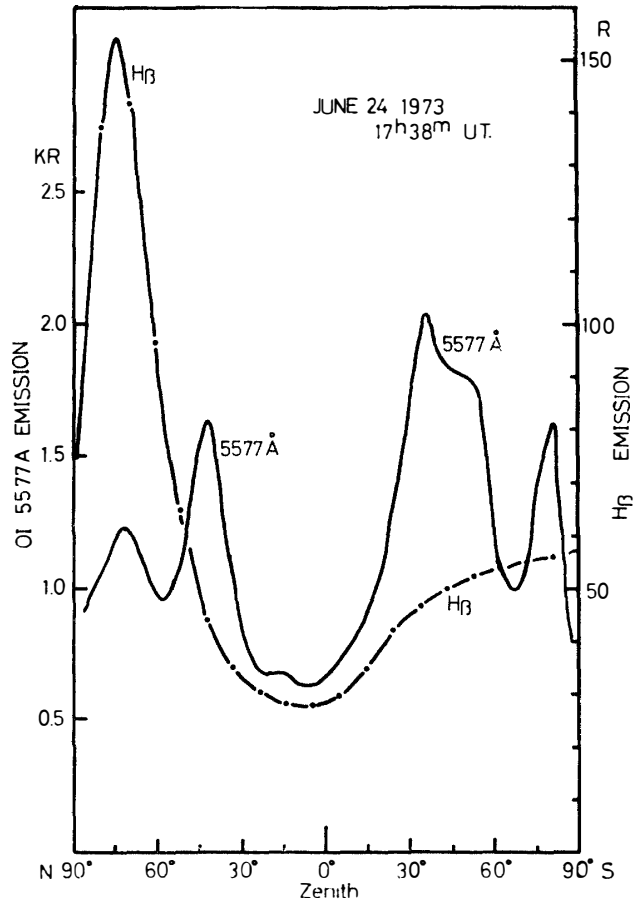


Fig. 11(b). Space distribution along the geomagnetic meridian of intensities of H_{β} 4861 Å and OI 5577 Å auroral emissions observed at Syowa Station at the practically same times as those for the auroral photographs in Fig. 11(a) ($Kp=5$).

belt above the southern horizon can be identified to a sharp peak of OI 5577 Å intensity.

Simultaneous data of three successive DAPP auroral photographs and corresponding all-sky camera ones are illustrated in Fig. 11(a). As seen in the DAPP photographs, the auroral oval was most expanded around 17^h38^m(UT) and began to contract in its polar radius during the period from 17^h38^m to 21^h00^m(UT). As shown in Fig. 11(a), the contraction of auroral oval radius results in a relative outgoing movement of Syowa Station (marked by SY in the figure) from just under the active discrete auroral belt at about 17^h18^m, through under the boundary region between the discrete and diffuse auroral belts at about 19^h19^m, to under the diffuse auroral belt at about 21^h00^m. The relative relationship of the location of Syowa Station to that of the auroral belts is clearly represented

also in a sequence of all-sky camera photographs obtained at Syowa Station (Fig. 11(a), bottom). At 17^h35^m–38^m, active discrete auroras are observed in most parts of the overhead sky, whereas a diffuse auroral belt is observed only above the equatorward horizon. At 19^h17^m–19^m, discrete auroras are observed in the poleward half sky and the equatorward parts of the sky are covered by diffuse auroras. Finally at 20^h58^m–21^h00^m, diffuse auroras are observed throughout the entire overhead sky of Syowa Station, no discrete aurora being detectable.

Fig. 11(b) which shows the distributions of H_{β} and OI 5577 Å intensities along the magnetic meridian at Syowa Station correspond, in time, to the DAPP and all-sky camera photographs at 17^h38^m shown in Fig. 11(a). In the all-sky camera photograph in Fig. 11(a), the magnetic meridian line through the zenith passes four comparatively bright discrete auroral arcs and a diffuse auroral belt near the northern horizon. Corresponding to the locations of the four discrete auroral arcs and the diffuse auroral belt respectively, four peaks of OI 5577 Å intensity and a peak of H_{β} one can be identified in Fig. 11(b).

Another example of successive simultaneous data of the DAPP auroral photographs and the all-sky camera ones and the scanning spectrophotometric data obtained at Syowa Station is given in Fig. 12. In Fig. 12(a), the diffuse auroral belt covers the overhead sky of Syowa Station during the period from 17^h21^m to 21^h00^m(UT), and no appreciable discrete auroras is observable. Corresponding to the observed result in the DAPP and all-sky camera photographs, simultaneous data of space distribution of H_{β} and OI 5577 Å intensities, given in Fig. 12(b) show that H_{β} auroral emissions are excited strongly in the southern sky at 17^h20^m and then the H_{β} emission area gradually expanded towards north, finally covering the entire sky at 20^h59^m. Throughout the whole period of the spectrophotometric recording, the intensity of OI 5577 Å line is kept at a very low level compared with that under the ordinary condition.

23 other sets of typical simultaneous auroral data of the DAPP and all-sky camera photographs and the scanning spectrophotometric data have been examined in a similar way. Throughout all results of such studies including the examples shown in Figs. 10 through 12, it has been concluded that the most parts of the diffuse auroral belt extending from the midnight sector to the evening one coincide with the proton auroral belt represented by the H_{β} emission belt, whereas the discrete auroras are identified to the electron auroras represented by the OI 5577 Å emission belts.

As far as the correlation of the geographical patterns and their moving characteristics between the discrete and diffuse auroral belts and those of the electron and proton auroral belts is concerned, therefore, the following correspondence can be concluded from the present study:

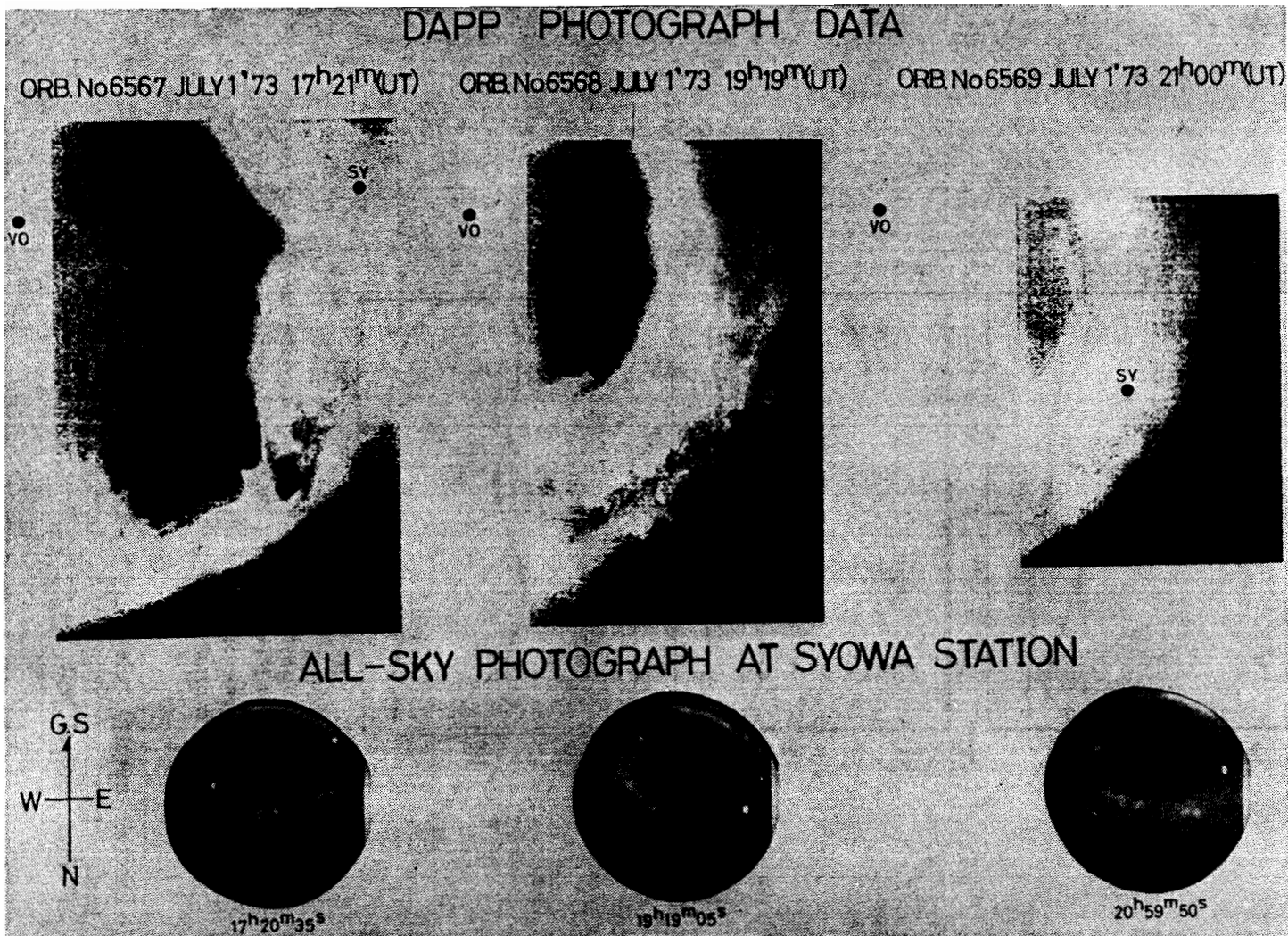


Fig. 12(a). Three successive DAPP auroral photographs and simultaneous all-sky camera photographs obtained at Syowa Station.

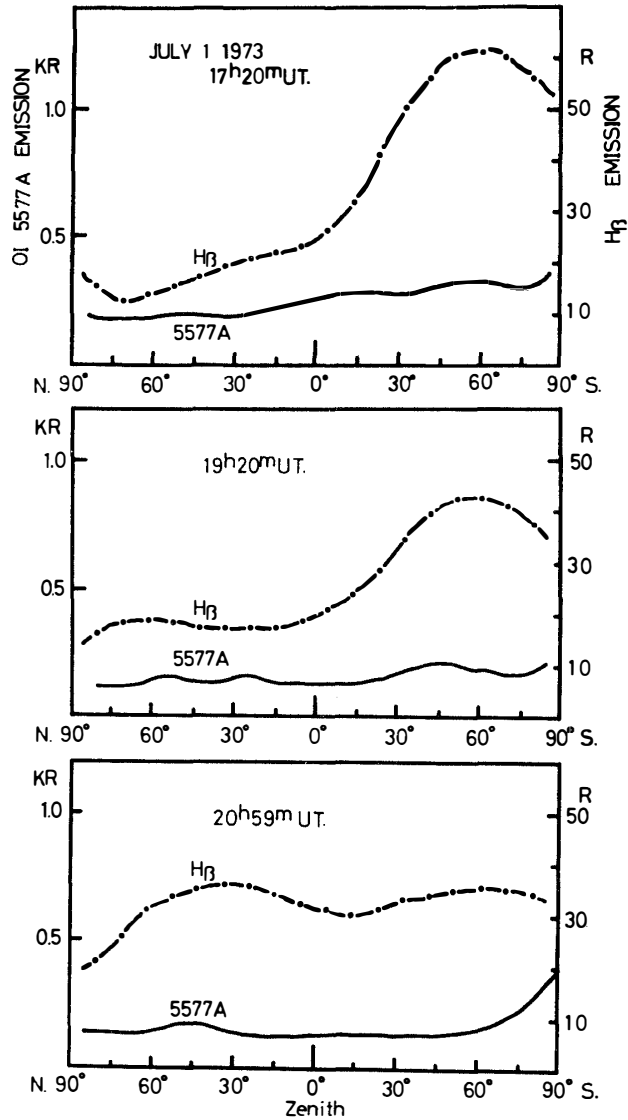
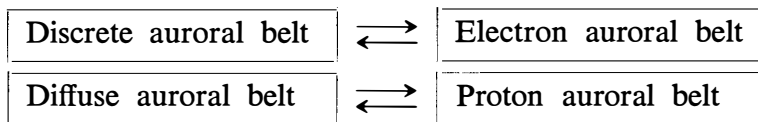


Fig. 12(b). Space distribution along the geomagnetic meridian of intensities of H_{β} 4861 Å and OI 5577 Å auroral emissions observed at Syowa Station at the practically same times as those for the auroral photographs in Fig. 12(a) ($Kp=4$).



6. Some Remarks and Acknowledgments

A remaining problem which has not yet been completely solved at the present stage may be the ratio of intensity of H_{β} emission to that of OI 5577 Å emission

in the spectrophotometric data in comparison with the ratio of diffuse auroral luminosity to discrete auroral one in the DAPP photographs. As seen in Figs. 10 through 12, the peak intensity of H_β emission is 10^2R in the order of magnitude whereas that of $OI\ 5577\ \text{\AA}$ emission is 1–2 KR. It seems likely, on the other hand, that the luminosity of diffuse auroral belts is several tenth of that of discrete auroral belts. As the emission of H_β line is always accompanied by H_α emission whose intensity is about five times as large as that of H_β emission and the DAPP photographic films are sufficiently sensitive to the wave length of H_α emission, the comparatively intense brightness of the diffuse auroral belt in the white aurora photographs could be interpreted as the sum of H_α - and H_β -luminosities. However, a direct experimental proof of this interpretation has not been given yet.

The authors wish to express their gratitude to all members of the 14th wintering party of Japanese Antarctic Research Expedition for their providing ground-based data of auroras obtained at Syowa Station in 1973. The aurora imaginary data of USAF-DAPP satellites were made available by the Air Weather Service through the National Geophysical and Solar-Terrestrial Center, EDS, NOAA, Boulder, Colorado. The authors' thanks are also due to the organization for supplying the DAPP auroral photograph data.

References

- AKASOFU, S.-I. (1964): The development of the auroral substorm. *Planet. Space Sci.*, **12**, 273–282.
- AKASOFU, S.-I. (1968): *Polar and Magnetospheric Substorms*. D. Reidel, Dordrecht, Netherlands, 280 pp.
- EATHER, R. H. and B. P. SANDFORD (1966): The zone of hydrogen emission in the night sky. *Aust. J. Phys.*, **19**, 25–33.
- FELDSTEIN, Y. I. (1963): Some problems concerning the morphology of auroras and magnetic disturbances at high latitudes. *Geomag. Aeron.*, **3**, 183–192.
- FELDSTEIN, Y. I. and G. V. STARKOV (1967): Dynamics of auroral belt and polar geomagnetic disturbances. *Planet. Space Sci.*, **15**, 209–229.
- FUKUNISHI, H. (1973): Dynamical morphology of proton aurora and electron aurora substorms and phenomenological model for magnetospheric substorms. *JARE Sci. Rep., Ser. A*, **11**, 77 pp.
- HIRASAWA, T. and T. NAGATA (1972): Constitution of polar substorm and associated phenomena in the southern polar region. *JARE Sci. Rep., Ser. A*, **10**, 76 pp.
- LUI, A. T. Y. and C. D. ANGER (1973): A uniform belt of diffuse auroral emission seen by the ISIS 2 scanning photometer. *Planet. Space Sci.*, **21**, 799–809.
- LUI, A. T. Y., P. PERRAUT, S.-I. AKASOFU and C. D. ANGER (1973): The diffuse aurora. *Planet. Space Sci.*, **21**, 857–861.
- PIKE, C. C. and J. A. WHALEN (1974): Satellite observations of auroral substorms. *J. Geophys. Res.*, **79**, 985–1000.
- SNYDER, A. L., S.-I. AKASOFU and T. N. DAVIS (1974): Auroral substorms observed from above the north polar region by a satellite. *J. Geophys. Res.*, **79**, 1393–1402.